

Optimizing soil analysis in precision agriculture: Evaluating alternative methods for SOC prediction

José Lizardo Reyna Bowen^{1*} , Lenin Vera Montenegro¹, María Isabel Delgado Moreira¹ 

¹ Escuela Superior Politécnica Agropecuaria de Manabí Manuel Félix López, Campus Politécnico El Limón, Calceta, Ecuador

* Corresponding author's e-mail: jlreyna@espam.edu.ec

ABSTRACT

Soil analysis plays a crucial role in precision agriculture, where alternatives or complementary methods to traditional laboratory analysis are needed to reduce costs and processing times. This study evaluated models from different devices for estimating soil organic carbon (SOC) using visible near-infrared (Vis-NIR) spectral data and examined the predictive performance of these models across diverse soil types and land uses. A total of 266 soil samples were collected at various depths from two dehesa farms. Soil reflectance spectra were measured using a LabSpec 5000 spectrophotometer with a contact probe and a Muglight accessory. SOC concentration was determined using the Walkley & Black method. Model prediction accuracy was assessed through metrics including the coefficient of determination (R^2), residual predictive deviation (RPD), root mean squared error (RMSE), and range error ratio (RER). Cross-validation demonstrated strong predictive accuracy for SOC, with R^2 and RPD values exceeding 0.95 and 4.54, respectively, and RER values surpassing 20. Although external validation metrics were more conservative, they still showed excellent RPD indices above 3.12, with no significant difference between devices. Both the Muglight and contact probe yielded low RMSE values (0.222 vs. 0.244) and high R^2 values (0.90 vs. 0.89). These findings indicate that both devices can reliably predict SOC, with the contact probe offering the added advantage of faster spectrum recording compared to the Muglight.

Keywords: soil fertility, precision agriculture, sustainable agriculture, spectral sensing, modeling.

INTRODUCTION

Soil organic carbon exhibits high spatial variability, making accurate estimates challenging (Arrouays et al., 2003). Precise SOC quantification is essential for identifying carbon sequestration potential. Traditional laboratory methods, while accurate, are costly and time-consuming (Bernoux et al., 2002). Visible and near-infrared (Vis-NIR) spectroscopy presents a promising alternative for rapid, non-destructive estimation of SOC. This method analyzes the spectral reflectance of soil samples within the visible (350–700 nm) and near-infrared (700–2500 nm) regions, enabling efficient SOC assessment across various soil types and conditions, researchers can identify specific wavelengths correlated with SOC content. Studies have demonstrated strong correlations between specific spectral regions and SOC.

For instance, the 700–800 nm region is linked to organic carbon (Wight et al., 2016), while wavelengths such as 490, 671, 785, 1090, 1420, 1860, and 2420 nm are associated with soil organic matter (SOM) (Ostovari et al., 2018). By leveraging these spectral signatures, Vis-NIR spectroscopy has the potential to revolutionize soil carbon monitoring and management.

Spectroscopy offers a cost-effective alternative to traditional methods like Walkley-Black, reducing costs by up to 90% through minimized sample handling and reagent use (Jackson et al., 2005; Marmette et al., 2018; Huang et al., 2011; Ji et al., 2016; Rossel et al., 2016). To effectively predict SOC using Vis-NIR, robust models are essential, often derived from extensive soil sample analysis using standard methods. Partial Least Squares Regression (PLSR) is a widely used technique (Wold et al., 2001); however, other

modeling approaches, including support vector machines (SVM), random forests (RF), multivariate adaptive regression splines (MARS), and classification and regression trees (CART), have also shown potential (He et al., 2007; Baldock et al., 2013; Minu and Shetty, 2018). Despite their promise, the generalizability of these models to new and geographically distinct regions remains an area of active investigation.

A rapid and non-destructive method for estimating SOC is Vis-NIR spectroscopy. However, the efficiency and accuracy of this technique are influenced by the type of device used to collect spectral information. Devices like trays and capsules require meticulous sample preparation, including filling, compacting, and cleaning, which can be time-consuming and prone to contamination. In contrast, contact probes simplify sample handling by directly measuring the spectral signal from the sample container. However, they may introduce errors due to inconsistent light incidence angles resulting from operator handling. The Muglight device, originally designed for raw material analysis, minimizes measurement errors caused by diffuse radiation. Nevertheless, it requires significantly more time for sample handling compared to contact probes. This study aims to compare the performance of models developed using data from different devices (trays, capsules, contact probes, and Muglight) to estimate SOC across diverse soil types and land uses.

MATERIALS AND METHODS

Location features

This study was conducted in Córdoba, Spain, at two Dehesa farms. Both farms share a common soil type: Eutric Cambisol. While both are primarily used for livestock grazing, they differ in specific land use practices. The first farm is dedicated solely to sheep grazing, with

occasional cultivation of vetch and oat mixtures on certain fields. The remaining areas are maintained as permanent pasture. In contrast, the second farm supports a more diverse livestock operation, including sheep, cattle, and pigs. Additionally, it has fewer cultivated fields, with the majority of the land designated as permanent pasture. A nearby abandoned field was included in the sampling area.

Soil samples

In March 2017, 266 soil samples were collected from the first farm. Sampling targeted areas beneath and outside tree canopies in both permanent pasture and corn-soybean rotation fields, at depths ranging from 0 to 60 cm. These samples were used to calibrate Vis-NIR models.

A total of 180 soil samples, at five different depths, were collected from the second farm in December 2017. Samples were obtained from fields subjected to high and moderate grazing intensities, as well as from an abandoned field. This dataset was utilized to validate the calibrated models' predictive ability on novel, unseen samples.

Soil carbon laboratory analysis

Soil samples from both farms were dried at 40 °C, sieved to 2 mm, and thoroughly homogenized. SOC concentrations were measured using the method described by Walkley (1947). The results of these analyses are described in Table 1.

Sample processing and spectroscopic analysis

Soil samples were oven-dried at 40 °C for 48 hours, sieved to 2 mm using a mechanical sieve shaker, and thoroughly homogenized. Spectral measurements (350–2500 nm) were acquired using a portable LabSpec 5000 spectrometer (ASD Inc., Boulder, CO, USA) equipped with a high-intensity halogen light source. For the first farm, both

Table 1. Descriptive statistics of SOC Concentration

Farm 1	n	SOC (%)	Std. Dev.	CV	Minimum	Maximum	Median
Total set	266	0.72	0.70	96.53	0.00	3.90	0.43
Calibration	216	0.72	0.71	98.85	0.00	3.90	0.43
Validation	50	0.73	0.64	87.10	0.02	2.21	0.49
Farm 2	n	SOC (%)	Std. Dev.	CV	Minimum	Maximum	Median
Total set	180	0.96	0.49	51.50	0.19	2.56	0.89

high intensity Muglight and contact probe measurements were collected in triplicate and quadruplicate, respectively. White reference scans were taken between each sample. The second farm's samples were exclusively measured with the Contact Probe using the same protocol (Figure 1).

Spectral data correction and predictive models

Raw spectral data were preprocessed using WinISI IV (version 4.6.8) to improve signal-to-noise ratios and remove spectral noise. The spectral range was reduced to 570–2450 nm to eliminate edge effects (Barnes et al., 1989). Standard normal variate (SNV) and SNV with detrending (SNV&D) were applied to enhance spectral quality (Wold et al., 2001). Partial least squares regression (PLSR) and modified partial least squares regression (PLSR-modified) were used to develop calibration models relating spectral data to soil organic carbon (SOC) concentrations (Martens et al., 1989; Terra et al., 2015).

Model assessment

The optimal model (PLSR or PLSR-modified with different spectral preprocessing techniques) was selected based on statistical metrics obtained from calibration and cross-validation processes (Huang et al., 2011; St. Luce et al., 2017). The standard SEC, calculated as the square root of the sum of squared residuals divided by the degrees of freedom ($n-p$), was a key metric. Cross-validation involved a four-fold random partitioning of the calibration dataset. Four models were developed, each using three-fourths of the data for training

and the remaining one-fourth for validation. The average R^2 and SEC values from these four iterations, denoted as 1-VR and SECV, respectively, were used to assess the model's predictive ability on independent datasets.

The SEC was calculated using Equation 1, where y_{ii} and y_i are the measured and predicted values of sample i , respectively, n is the number of samples, and p is the number of PLSR variables used by the model.

$$SEC = \sqrt{\sum_{i=1}^n \frac{(y_{ii} - y_i)^2}{n-p-1}} \quad (1)$$

To assess model performance, the range error ratio (RER) and the ratio of performance to deviation (RPD), two commonly used metrics in spectral data analysis, were calculated as defined in Equations 2 and 3.

$$RER = \frac{(Min-Max)}{SEC} \quad (2)$$

$$RPD = \frac{SD}{SEC} \quad (3)$$

Model performance was evaluated using the range error ratio (RER) and the ratio of performance to deviation (RPD) (Roberts et al., 2004; Pinheiro et al., 2017). RER values exceeding 20 and RPD values greater than 2.5 indicate excellent model performance. External validation was conducted on a 20% subset of the first farm's soil samples. The root mean square error (RMSE), calculated as the square root of the sum of squared residuals divided by the number of samples (Equation 4), was used to assess the model's predictive accuracy. Additionally, RER and RPD were calculated for the validation set. Finally, the SOC content of the second farm's soil samples was predicted using their spectra and the selected

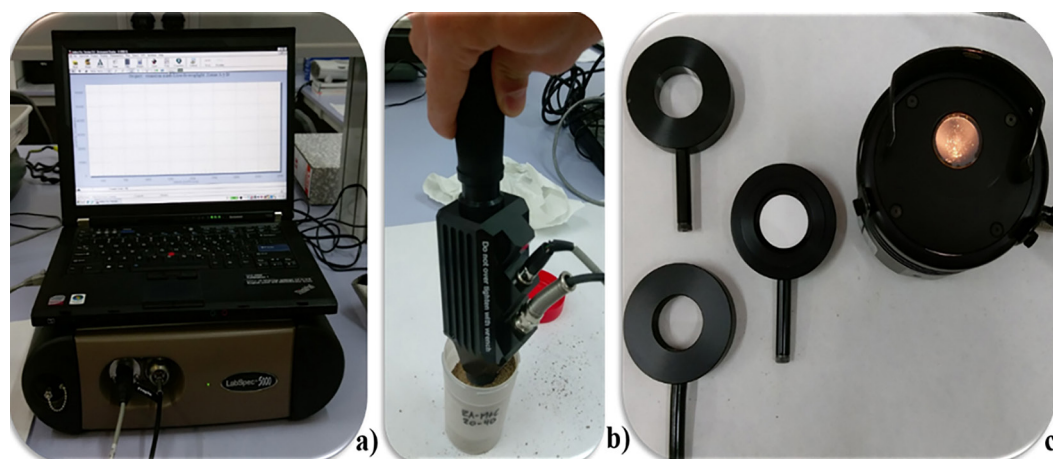


Figure 1. Instruments employed in this study included: a) LabSpec 5000 spectrometer (Analytical Spectral Devices, Inc., Boulder, CO, USA), b) contact-probe sensor, c) Muglight sensor

best model. RMSE was employed to evaluate the model's performance on this independent dataset.

$$RMSE = \sqrt{\sum_{i=1}^n \frac{(y_{ii} - y_i)^2}{n}} \quad (4)$$

RESULTS

Soil spectral reflectance variability with depth

Reflectance spectra were analyzed within the 570–2450 nm range. In general, the contact-probe device yielded lower reflectance values compared to the Muglight, likely due to the Muglight's larger lighting window diameter (Figure 2a). However, both devices produced spectra with similar overall shapes, differing primarily in the magnitude of reflectance (Figure 2b).

Analysis of the 216 soil samples scanned with both sensors revealed distinct spectral patterns. The upper soil layers (0–2, 2–5, 5–10, and 10–20 cm), which had higher SOC content, exhibited greater reflectance, whereas the deeper layers (40–60, 60–80, and 80–100 cm) with lower SOC content showed reduced reflectance (Figure 3). A closer examination of the first sample group, focusing on layers with similar clay content (0–2, 2–5, 5–10, and 10–20 cm), provided further insights into the relationship between SOC and spectral response, which revealed a clear stratification in soil profile carbon content, which was reflected in the spectral data (Figure 3a). Reflectance was lowest in shallow samples with high carbon content and increased with depth where carbon content was lower. In contrast, samples without the canopy influence showed higher reflectance in deeper

layers, indicating lower organic carbon content (Figure 3b). Samples under adult tree canopies exhibited similar organic carbon contents across depths, leading to consistent spectral lines, while samples outside canopy influence displayed spectral variations and lower carbon stratification (Figure 3c).

Figure 4 shows the first derivative reflectance spectra of soil at various depths, as recorded by both sensors. The spectra exhibit similar first derivative patterns across devices, with prominent absorption features around 1400 nm, 1900 nm, and 2200 nm, which are indicative of soil organic matter content.

Calibration and prediction of SOC

Calibration with both sensors yielded favorable results, aligning well with the observed ranges of soil carbon percentages. Regardless of the device used for spectral acquisition, all models performed well, with the PLSR-modified model demonstrating superior performance in predicting organic carbon values. Notably, spectral preprocessing contributed to enhanced calibration models, as evidenced by R², SEC, 1-VR, SEVC, RDP and RER (quality indicators), displaying excellence in both calibration and validation (Table 2). Predictions of SOC proved to be excellent for both devices, with the Muglight sensor achieving an R² of 0.90 and the Contact-Probe sensor obtaining an R² of 0.892. Figure 5 illustrates the striking similarity in predictions between the two devices. However, results from farm 2 revealed a slightly lower SOC prediction with an R² value of 0.656 compared to that of the first farm (see Figure 6).

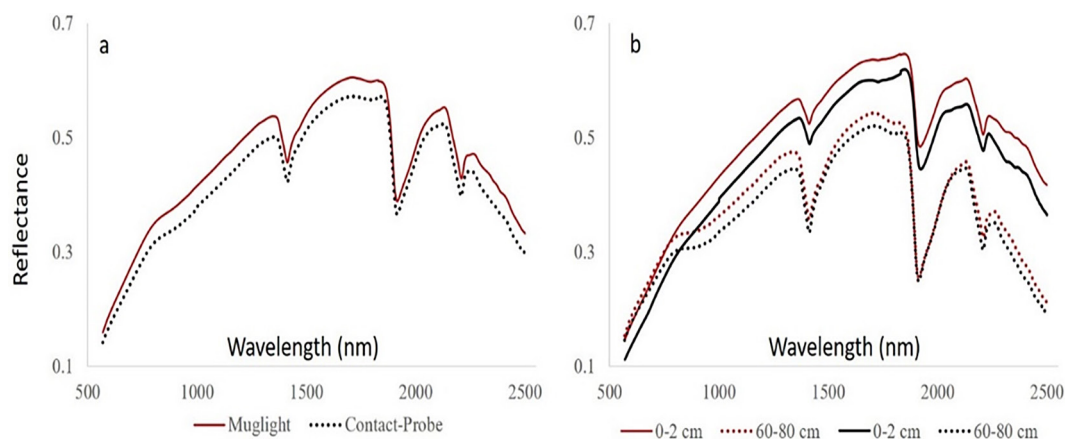


Figure 2. Average spectral curves of soil samples from Farm 1, measured with Muglight (continuous line) and contact probe (segmented line) sensors: a) total soil depth, b) comparison of 0–2 cm and 60–80 cm depths.

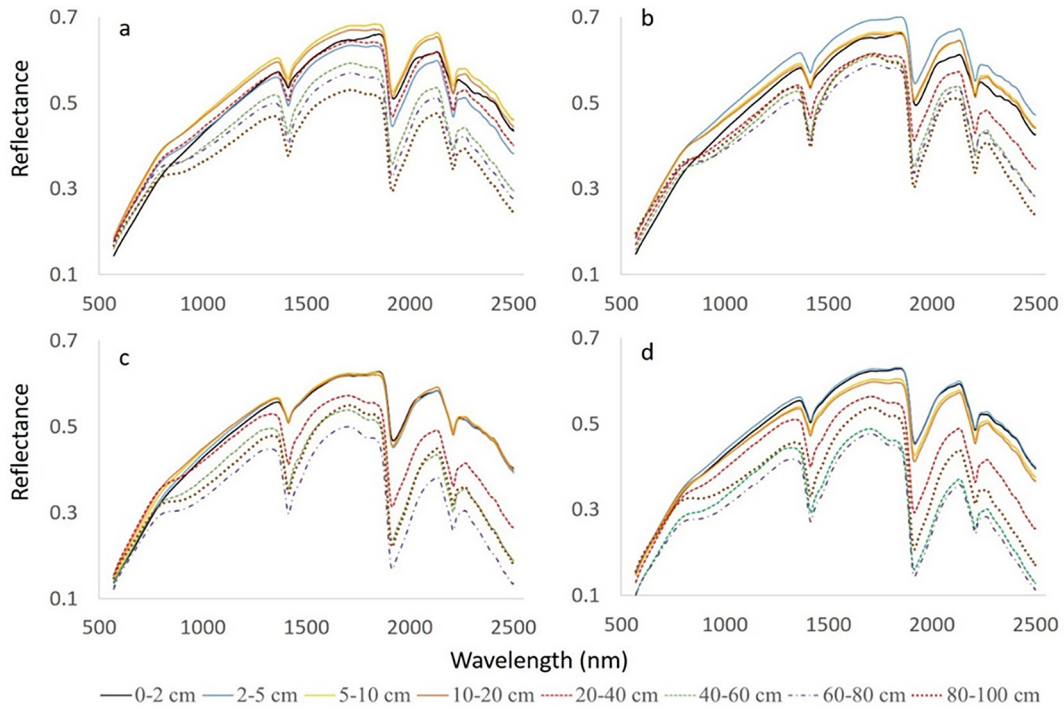


Figure 3. Soil reflectance spectra from Farm 1. The specific locations include: a) Pasture area beneath the canopy of a young Holm oak tree, b) Pasture area outside the canopy of a young Holm oak tree, c) Pasture-crop area beneath the canopy of a mature Holm oak tree, d) Pasture-crop area outside the canopy of a mature Holm oak tree

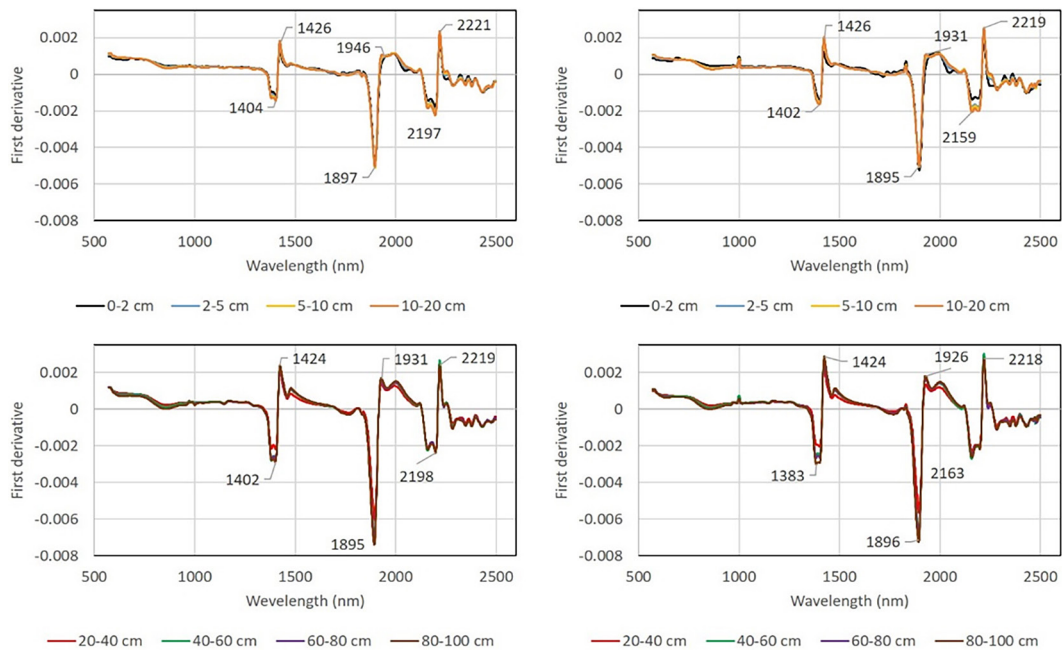


Figure 4. Average first-derivative spectra of soil samples from different depths: (left) Muglight sensor, (right) contact probe sensor

DISCUSSION

Remarkably, reflectance peaks and curve shapes remained consistent across both devices, aligning with findings from Guillén et al. (2013).

These results suggest that the contact-probe device can provide comparable reflectance measurements to those obtained in our study. Previous research has consistently demonstrated a negative correlation between carbon content and reflectance (Guillén

Table 2. Calibration model performance for contact probe and Muglight sensors. Performance metrics of the calibration models, including the coefficient of determination (R^2), root mean square error (RMSE), ratio of performance to deviation (RPD), range error ratio (RER), and cross-validation (1-VR)

Sensor	Regression	Spectral preprocessing		n	Mean	Range	Std.	SEC	R^2	SEVC	1-VR	RPD	RER
Contact-probe	PLSR - modified	SNV	1,4,4,1	200	0.642	0.00–3.90	0.616	0.110	0.968	0.124	0.959	5.0	31.37
Muglight	PLSR - modified	SNV&D	1,10,5,1	198	0.589	0.00–2.46	0.509	0.089	0.969	0.112	0.952	4.5	21.88

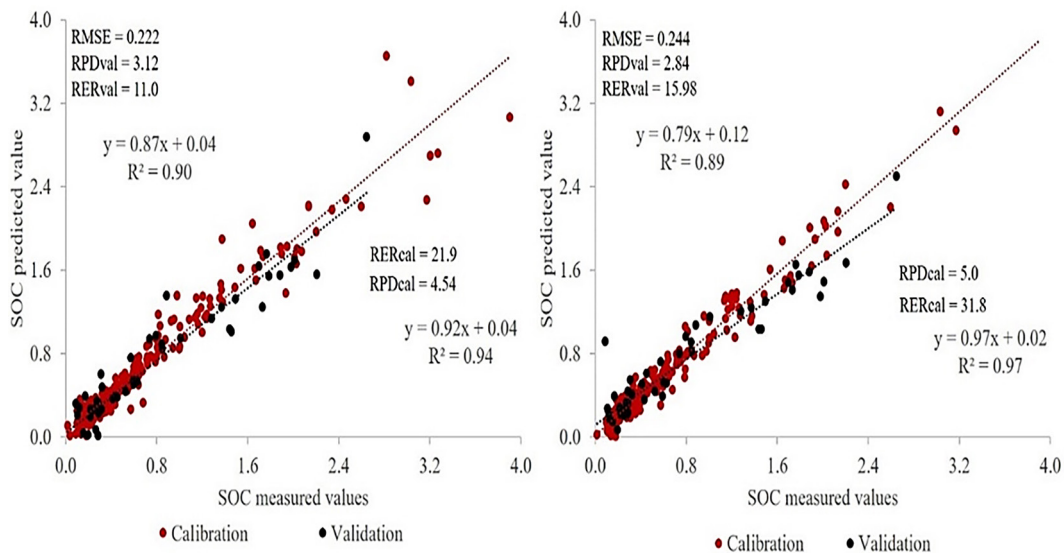


Figure 5. Correlation between measured and predicted SOC: (left) contact probe sensor, (right) Muglight sensor

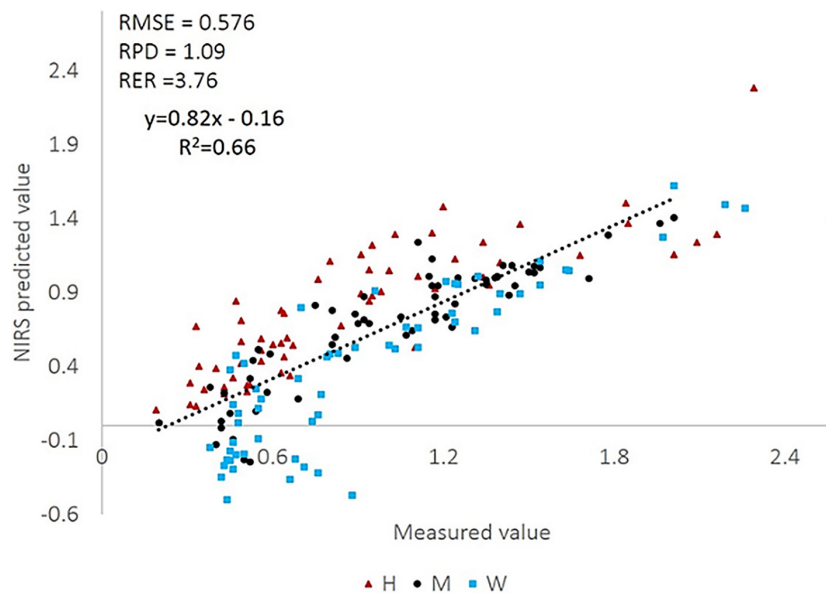


Figure 6. Correlation between measured and predicted SOC using the contact probe sensor. The samples were collected from fields with different grazing intensities: without grazing (W), moderate (M) and high (H)

et al., 2013; Omran et al., 2017; Xu et al., 2018; Kusumo et al., 2018). Additionally, soil mineralogy, particularly clay content, can significantly influence reflectance curves, with higher clay content

leading to lower reflectance (Stenberg et al., 2010; Siirt et al., 2016; Kusumo et al., 2018; Omran et al., 2017). However, factors such as soil management practices and tree presence can alter organic carbon

content and, consequently, affect spectral curve behavior. In our study, variations in spectral curves were primarily attributed to differences in clay, silt, and sand content rather than organic carbon variations. For example, the spectral curve for the 20–40 cm soil sample, which lies between deeper and shallower samples, reflects the higher clay content observed in deeper sections of the soil profile.

The absorption feature within the range of 350–1.000 nm is likely attributed to Fe oxides, specifically hematite and goethite, while wavelengths between 1.000 and 2.500 nm are influenced by clay minerals and organic matter (Rosset et al., 2010). First-derivative reflectance spectra (Figure 4) revealed distinct absorption peaks at 1400, 1900, and 2200 nm, associated with C-H, O-H, and C-O combinations, respectively. These findings align with previous research linking soil carbon content and mineralogy (Omran et al., 2017; Xu et al., 2018; Douglas et al., 2018; Chen et al., 2016; Kusumo et al., 2018; Chen et al., 2019). Additionally, a minor absorption peak around 2200 nm was associated with the Al-OH absorption band of clay minerals (Clark et al., 1990). However, while slight spectral shape differences were observed across the range, soil composition, particularly texture, played a significant role in influencing spectral variability and potentially masked expected trends. For instance, higher carbon content samples were not consistently associated with lower reflectance throughout the entire sample set, likely due to the impact of soil texture.

Various models calibrated for different soil types have demonstrated R^2 values ranging from 0.75 to 0.99 (Douglas et al., 2018; Kusumo et al., 2018a; Kusumo et al., 2018b; St. Luce et al., 2017; Hosseini et al., 2017; Minu and Shetty, 2018). Pinheiro et al. (2017) achieved similar results with $R^2 = 0.85$ and $RPD = 2.58$ using 200 calibration samples. Our results, obtained using two sensors (contact-probe: $R^2 = 0.89$, $RMSE = 0.244$, $RPD = 2.484$; Muglight: $R^2 = 0.90$, $RMSE = 0.222$, $RPD = 3.12$), fall within the higher range of performance, indicating the successful application of the PLSR-modified model, as noted by Gandariasbeitia et al. (2017) and Guillén et al. (2013).

While PLSR prediction models can be effectively calibrated for various soil types, predicting carbon content in the second farm, which had the same soil type but different management practices (intensive, moderate, and no grazing), yielded poor results. This aligns with previous findings

(Guillén et al., 2013; Makovníková et al., 2017; O'Rourke et al., 2011). Although soil cover management did not significantly affect spectral properties in our study, incorporating soil spectral signatures from diverse management types could enhance model robustness and applicability across various scenarios.

Our results highlight the significant influence of soil mineralogical composition on reflectance spectra, which can significantly impact model performance, especially in low-carbon soils. This can lead to inconsistencies in predictions. Additionally, temporal fluctuations in soil moisture can compromise the predictive capabilities of Vis-NIR spectroscopy models for estimating SOC (McGuirk & Cairns, 2024). Soil moisture significantly influences soil reflectance, particularly in the Vis-NIR range, due to water's distinct absorption features. Higher moisture content can attenuate reflectance and distort spectral properties, potentially masking or interfering with the spectral signatures associated with organic carbon (Hong et al., 2017).

Consequently, temporal fluctuations in soil moisture can alter reflectance data, potentially leading the model to misinterpret these variations, thereby diminishing predictive accuracy (Cao et al., 2020). To mitigate this, models frequently use preprocessing techniques to normalize or correct for moisture variation. Additionally, specialized algorithms may be employed to differentiate spectral features associated with SOC from those linked to water content. Integrating moisture corrections or incorporating moisture as a covariate within the model could enhance robustness across varying moisture conditions.

CONCLUSIONS

The equations generated results with excellence indices, signifying the adeptness of both types of equipment in accurately predicting organic carbon concentration. Particularly noteworthy was the precise prediction achieved with the contact-probe, which not only delivered accurate results but also expedited the spectrum recording process. However, to further bolster the accuracy and robustness of these predictive models, it's imperative to consider incorporating samples from analogous soils sourced from diverse geographical regions into the calibration dataset. By accounting for the variability inherent in soil types across different areas, we

can refine and enhance the predictive capabilities of these models. Moreover, it's crucial to recognize that while organic matter content undoubtedly plays a role in shaping soil sample spectra, our findings underscore the greater potential impact of soil mineralogy on spectral variations. This insight underscores the need for a nuanced understanding of the factors influencing soil spectral properties to optimize the efficacy of predictive modeling in soil science applications.

Acknowledgments

The authors would like to thank administrative and technical support of the institutions that were part of the research. This research was funded by P12-AGR-0931 (Andalusian Government), RTA2014-00063-C04-03 (Spanish Government), SHui (European Commission Grant Agreement number: 773903) and EU-FEDER funds, whose support is gratefully acknowledged.

REFERENCES

1. Arrouays D., Feller C., Jolivet C., Saby N., Andreux F., Bernoux M. (2003). Estimation de stocks de carbone organique des sols à différentes échelles d'espace et de temps. *Etude et Gestion des Sols*, 10(4), 347–355.
2. Baldock J. A., Hawke B., Sanderman J., MacDonal L. M. (2013). Predicting contents of carbon and its component fractions in Australian soils from diffuse reflectance mid-infrared spectra. *Soil Research*, 51(7–8), 577–595. <https://doi.org/10.1071/SR13077>
3. Barnes R. J., Dhanoa M. S., Lister S. J. (1989). Standard normal variate transformation and detrending of near-infrared diffuse reflectance spectra. *Applied Spectroscopy*, 43(5), 772–777. <https://doi.org/10.1366/0003702894202201>
4. Bernoux M., da Conceição M., Volkoff B., Cerri C. C. (2002). Brazil's Soil Carbon Stocks. *Soil Science Society of America Journal*, 66(3). <https://doi.org/10.2136/sssaj2002.8880>
5. Cao Y., Bao N., Liu S., Zhao W., Li S. (2020). Reducing moisture effects on soil organic carbon content prediction in visible and near-infrared spectra with an external parameter orthogonalization algorithm. *Canadian Journal of Soil Science*, 1–10. [dx.doi.org/10.1139/cjss-2020-0009](https://doi.org/10.1139/cjss-2020-0009)
6. Chen S., Li S., Ma W., Ji W., Xu D., Shi Z., & Zhang G. (2019). Rapid determination of soil classes in soil profiles using vis-NIR spectroscopy and multiple objectives mixed support vector classification. *European Journal of Soil Science*, 70(1), 42–53. <https://doi.org/10.1111/ejss.12715>
7. Chen S., Peng J., Ji W., Zhou Y., He J., Shi Z. (2016). Study on the characterization of VNIR-MIR spectra and prediction of soil organic matter in paddy soil. *Guang Pu Xue Yu Guang Pu Fen Xi = Guang Pu*, 36(6), 1712–1716. <http://www.ncbi.nlm.nih.gov/pubmed/30052377>
8. Clark R. N., King T. V., Klejwa M., Swayze G. A., Vergo N. (1990). High spectral resolution reflectance spectroscopy of minerals. *Journal of Geophysical Research*, 95. <https://doi.org/10.1029/jb095ib08p12653>
9. Douglas R. K., Nawar S., Alamar M. C., Coulon F., Mouazen A. M. (2018). Rapid detection of alkanes and polycyclic aromatic hydrocarbons in oil-contaminated soil with visible near-infrared spectroscopy. *European Journal of Soil Science*, 1–11. <https://doi.org/10.1111/ejss.12567>
10. Gandariasbeitia M., Besga G., Albizu I., Larregla S., Mendarte S. (2017). Prediction of chemical and biological variables of soil in grazing areas with visible- and near-infrared spectroscopy. *Geoderma*, 305, 228–235. <https://doi.org/10.1016/j.geoderma.2017.05.045>
11. Guillén C. E., Dávila M. J., Gilliot J. M., Vaoudour E. (2013). Aporte de la espectroscopia a la estimación de carbono orgánico de los suelos de la planicie de Versailles, Francia. *Revista Geografica Venezolana*, 54(1), 85–98.
12. He Y., Huang M., Garcia A., Hernandez A., Song H. (2007). Prediction of soil macronutrients content using near-infrared spectroscopy. *Computers and Electronics in Agriculture*, 58(2), 144–153. <https://doi.org/10.1016/j.compag.2007.03.011>
13. Hong Y., Yu L., Chen Y., Liu Y., Liu Y., Liu Y., Cheng H. (2017). Prediction of soil organic matter by VIS-NIR spectroscopy using normalized soil moisture index as a proxy of soil moisture. *Remote Sensing*, 10(1), 28. <https://doi.org/10.3390/rs10010028>
14. Hosseini M., Rajabi S., Khaledian Y., Jafarzadeh H., Brevik E., Movahedi S. (2017). Comparison of multiple statistical techniques to predict soil phosphorus. *Applied Soil Ecology*, 114, 123–131. <https://doi.org/10.1016/j.apsoil.2017.02.011>
15. Huang C., Han L., Liu X., Ma L. (2011). The rapid estimation of cellulose, hemicellulose, and lignin contents in rice straw by near infrared spectroscopy. *Energy Sources, Part A: Recovery, Utilization and Environmental Effects*, 33(2), 114–120. <https://doi.org/10.1080/15567030902937127>
16. Ji W., Li S., Chen S., Shi Z., Viscarra Rossel R. A., Mouazen A. M. (2016). Prediction of soil attributes using the Chinese soil spectral library and standardized spectra recorded at field conditions.

- Soil and Tillage Research*, 155, 492–500. <https://doi.org/10.1016/j.still.2015.06.004>
17. Kusumo B. H. (2018). In Situ Measurement of Soil Carbon with Depth using Near Infrared (NIR) Spectroscopy. *IOP Conference Series: Materials Science and Engineering*, 434. <https://doi.org/10.1088/1757-899X/434/1/012235>
 18. Kusumo B. H., Sukartono S., Bustan B. (2018a). The rapid measurement of soil carbon stock using near-infrared technology. *IOP Conference Series: Earth and Environmental Science*, 129(1). <https://doi.org/10.1088/1755-1315/129/1/012023>
 19. Kusumo B. H., Sukartono S., Bustan B. (2018b). Rapid measurement of soil carbon in rice paddy field of lombok island indonesia using near infrared technology. *IOP Conference Series: Materials Science and Engineering*, 306(1). <https://doi.org/10.1088/1757-899X/306/1/012014>
 20. McGuirk S. L., Cairns I. H. (2024). Relationships between soil moisture and visible–NIR soil reflectance: A review presenting new analyses and data to fill the gaps. *Geotechnics*, 4(1), 78–108. <https://doi.org/10.3390/geotechnics4010005>
 21. Makovníková J., Širáň M., Houšková B., Pálka B., Jones A. (2017). Comparison of different models for predicting soil bulk density. *Case study – Slovakian agricultural soils. International Agrophysics*, 31(4), 491–498. <https://doi.org/10.1515/intag-2016-0079>
 22. Marion L. (1969). Soil chemical analysis: advanced course: a manual of methods useful for instruction and research in soil chemistry, physical chemistry of soils, soil fertility, and soil genesis. (available at <http://www.sidalc.net/cgi-bin/wxis.exe/?IsisScript=bac.xis&method=post&formato=2&cantidad=1&expresion=mfn=029021>)
 23. Marmette M., Adamchuk V., Nault J., Tabatabai S., Cocciardi R. (2018). Comparison of the Performance of Two Vis-NIR Spectrometers in the Prediction of Various Soil Properties. *Proceedings of the 14th International Conference on Precision Agriculture, Montreal, Quebec, Canada*, (June), 1–12. (available at <https://www.ispag.org/proceedings/?action=abstract&id=5404&search=types>)
 24. Martens H., Naes T. (1989). Assessment, validation and choice of calibration method. *Multivariate Calibration*: 237–266.
 25. Minu S., Shetty A. (2018). Prediction accuracy of soil organic carbon from ground based visible near-infrared reflectance spectroscopy. *Journal of the Indian Society of Remote Sensing*. <https://doi.org/10.1007/s12524-017-0744-0>
 26. O'Rourke S. M., Holden N. M. (2011). Optical sensing and chemometric analysis of soil organic carbon - a cost effective alternative to conventional laboratory methods? *Soil Use and Management*. <https://doi.org/10.1111/j.1475-2743.2011.00337.x>
 27. Omran S. (2017). Rapid soil analyses using modern sensing technology: toward a more sustainable agriculture. In *The Handbook of Environmental Chemistry*, 41–53. <https://doi.org/10.1007/698>
 28. Ostovari Y., Ghorbani-Dashtaki S., Bahrami H., Abbasi M., Dematte A. M., Arthur E., Panagos P. (2018). Towards prediction of soil erodibility, SOM and CaCO₃ using laboratory Vis-NIR spectra: A case study in a semi-arid region of Iran. *Geoderma*, 314, 102–112. <https://doi.org/10.1016/j.geoderma.2017.11.014>
 29. Ouerghemmi W., Gomez C., Naceur S., Lagacherie P. (2011). Applying blind source separation on hyperspectral data for clay content estimation over partially vegetated surfaces. *Geoderma*, 163(3–4), 227–237. <https://doi.org/10.1016/j.geoderma.2011.04.019>
 30. Pinheiro É., Ceddia M., Clingensmith C., Grunwald S., Vasques G. (2017). Prediction of soil physical and chemical properties by visible and near-infrared diffuse reflectance spectroscopy in the central amazon. *Remote Sensing*, 9(4). <https://doi.org/10.3390/rs9040293>
 31. Roberts C., Workman J., Reeves J. 2004. Near-infrared spectroscopy in agriculture. *Agronomy*, 44, 1–14.
 32. Rossel R., Behrens T. (2010). Using data mining to model and interpret soil diffuse reflectance spectra. *Geoderma*, 158(1–2), 46–54. <https://doi.org/10.1016/j.geoderma.2009.12.025>
 33. Siirt M. B., Species I. P. (2016). Visible and near infrared spectroscopy techniques for determination of some physical and chemical properties in Kazova. Visible and Near Infrared Spectroscopy Techniques for Determination of Some Physical and Chemical Properties in Kazova Watershed. *Advances in Environmental Biology*, 10, 61–72.
 34. St. Luce M., Ziadi N., Gagnon B., Karam A. (2017). Visible near infrared reflectance spectroscopy prediction of soil heavy metal concentrations in paper mill biosolid- and liming by-product-amended agricultural soils. *Geoderma*, 288, 23–36. <https://doi.org/10.1016/j.geoderma.2016.10.037>
 35. Stenberg B., Viscarra Rossel R. A., Mouazen A. M., Wetterlind J. (2010). Visible and near infrared spectroscopy in soil science. *Advances in Agronomy* (107). [https://doi.org/10.1016/S0065-2113\(10\)07005-7](https://doi.org/10.1016/S0065-2113(10)07005-7)
 36. Terra F. S., Demattê J., Viscarra Rossel R. A. (2015). Spectral libraries for quantitative analyses of tropical Brazilian soils: Comparing vis-NIR and mid-IR reflectance data. *Geoderma*, 255, 81–93. <https://doi.org/10.1016/j.geoderma.2015.04.017>
 37. Viscarra Rossel R. A., Behrens T., Ben-Dor E., Brown D. J., Demattê J. A., Shepherd K. D., Shi Z., Stenberg B., Stevens A., Adamchuk V., Aichi H., Barthès B. G., Bartholomeus H. M., Bayer A.

- D., Bernoux M., Böttcher K., Brodský L., Du C. W., Chappell A., Ji, W. (2016). A global spectral library to characterize the world's soil. *Earth-Science Reviews*, 155, 198–230. <https://doi.org/10.1016/j.earscirev.2016.01.012>
38. Viscarra Rossel R. A., Walvoort D., McBratney A. B., Janik L. J., Skjemstad J. O. (2006). Visible, near infrared, mid infrared or combined diffuse reflectance spectroscopy for simultaneous assessment of various soil properties. *Geoderma*, 131(1–2), 59–75. <https://doi.org/10.1016/j.geoderma.2005.03.007>
39. Vitharana U., Mishra U., Mapa R. B. (2019). National soil organic carbon estimates can improve global estimates. *Geoderma*, 337, 55–64. <https://doi.org/10.1016/j.geoderma.2018.09.005>
40. Walkley A. (1947). A critical examination of a rapid method for determining organic carbon in soils—effect of variations in digestion conditions and of inorganic soil constituents. *Soil Science*, 63, 251–264. <https://doi.org/10.1097/00010694-194704000-00001>
41. Wenjun J., Zhou S., Jingyi H., Shuo L. (2014). In situ measurement of some soil properties in paddy soil using visible and near-infrared spectroscopy. *PLoS ONE*. <https://doi.org/10.1371/journal.pone.0105708>
42. Wight P., Allen L., Tyler D., Labbe, N., Rials T., Ashworth A. (2016). Comparison of near infrared reflectance spectroscopy with combustion and chemical methods for soil carbon measurements in agricultural soils. *Communications in Soil Science and Plant Analysis*, 47(6), 731–742. <https://doi.org/10.1080/00103624.2016.1146750>
43. Wold S., Sjöström M., Eriksson L. (2001). PLS-regression: a basic comp with MR. *Chemometrics and Intelligent Laboratory Systems*, 58(2), 109–130. [https://doi.org/10.1016/S0169-7439\(01\)00155-1](https://doi.org/10.1016/S0169-7439(01)00155-1)
44. Xu D., Ma W., Chen S., Jiang Q., He K., Shi Z. (2018). Assessment of important soil properties related to Chinese Soil Taxonomy based on vis–NIR reflectance spectroscopy. *Computers and Electronics in Agriculture*, 144, 1–8. <https://doi.org/10.1016/j.compag.2017.11.029>
45. Xu S., Zhao Y., Wang M., Shi X. (2018). Comparison of multivariate methods for estimating selected soil properties from intact soil cores of paddy fields by Vis–NIR spectroscopy. *Geoderma*, 310, 29–43. <https://doi.org/10.1016/j.geoderma.2017.09.013>